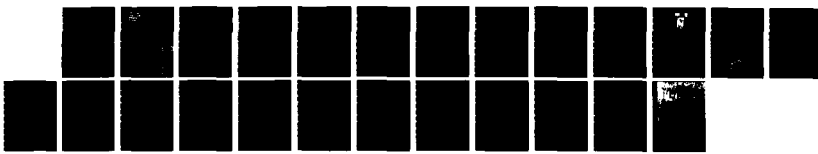
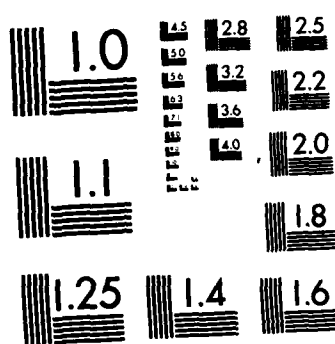


AD-A134 729 THE EFFECT OF GAS BUBBLES AND CAVITY DIMENSIONS ON THE 1/1
LOCAL ELECTRODE PO. (U) PENNSYLVANIA STATE UNIV
UNIVERSITY PARK DEPT OF MATERIALS SCI. H W PICKERING
UNCLASSIFIED 07 NOV 83 N00014-81-K-0025 F/G 11/6 NL





MICROCOPY RESOLUTION TEST CHART
NATIONAL BUREAU OF STANDARDS-1963-A

**COLLEGE OF
EARTH AND
MINERAL
SCIENCES**

12

DEPARTMENT OF MATERIALS SCIENCE
METALLURGY PROGRAM

AD-A134 729

*TECHNICAL REPORT

November 1983

OFFICE OF NAVAL RESEARCH

Contract No. N000-14-81-K-0025

THE EFFECT OF GAS BUBBLES AND CAVITY DIMENSIONS ON THE LOCAL
ELECTRODE POTENTIAL WITHIN PITS, CREVICES AND CRACKS

H. W. Pickering

Department of Materials Science and Engineering
The Pennsylvania State University
University Park, Pennsylvania 16802

64C43 5N

DTIC
ELECTED
S NOV 15 1983
A

Reproduction in whole or in part is permitted for any purpose of the
United States Government. Distribution of this document is unlimited.

DTIC FILE COPY

**The Pennsylvania
State University
University Park,
Pennsylvania**



83 11 10 039

THE PENNSYLVANIA STATE UNIVERSITY

College of Earth and Mineral Sciences

UNDERGRADUATE PROGRAMS OF STUDY

Ceramic Science and Engineering, Earth Sciences, Fuel Science, Geography, Geosciences, Metallurgy, Meteorology, Mineral Economics, Mining Engineering, Petroleum and Natural Gas Engineering, and Polymer Science.

GRADUATE PROGRAMS AND FIELDS OF RESEARCH

Ceramic Science, Fuel Science, Geochemistry and Mineralogy, Geography, Geology, Geophysics, Metallurgy, Meteorology, Mineral Economics, Mineral Processing, Mining Engineering, Petroleum and Natural Gas Engineering, and Polymer Science.

**UNIVERSITY-WIDE INTERDISCIPLINARY GRADUATE PROGRAMS INVOLVING E&MS
FACULTY AND STUDENTS**

Earth Sciences, Ecology, Environmental Pollution Control Engineering, Mineral Engineering Management, Operations Research, Regional Planning, and Solid State Science.

ASSOCIATE DEGREE PROGRAMS

Metallurgical Engineering Technology and Mining Technology.

INTERDISCIPLINARY RESEARCH GROUPS WITHIN THE COLLEGE

Coal Research Section, Mineral Conservation Section, Ore Deposits Research Section, and Mining and Mineral Resources Research Institute.

ANALYTICAL AND STRUCTURE STUDIES

Classical chemical analysis of metals and silicate and carbonate rocks; X-ray crystallography; electron microscopy and diffraction; electron microprobe analysis; atomic absorption analysis; spectrochemical analysis.

SECURITY CLASSIFICATION OF THIS PAGE (When Data Entered)

REPORT DOCUMENTATION PAGE		READ INSTRUCTIONS BEFORE COMPLETING FORM
1. REPORT NUMBER Technical Report	2. GOVT ACCESSION NO.	3. RECIPIENT'S CATALOG NUMBER
4. TITLE (and Subtitle) The Effect of Gas Bubbles and Cavity Dimensions on the Local Electrode Potential within Pits, Crevices and Cracks		5. TYPE OF REPORT & PERIOD COVERED Technical Report
7. AUTHOR(s) H. W. Pickering		6. PERFORMING ORG. REPORT NUMBER
9. PERFORMING ORGANIZATION NAME AND ADDRESS Metallurgy Program, 209 Steidle Building The Pennsylvania State University University Park, PA 16802		10. PROGRAM ELEMENT, PROJECT, TASK AREA & WORK UNIT NUMBERS
11. CONTROLLING OFFICE NAME AND ADDRESS Metallurgy Branch Office of Naval Research Arlington, VA 22217		12. REPORT DATE November 7, 1983
14. MONITORING AGENCY NAME & ADDRESS (if different from Controlling Office)		13. NUMBER OF PAGES
		15. SECURITY CLASS. (of this report)
		15a. DECLASSIFICATION/DOWNGRADING SCHEDULE
16. DISTRIBUTION STATEMENT (of this Report) Distribution of this document is unlimited		
17. DISTRIBUTION STATEMENT (of the abstract entered in Block 20, if different from Report)		
18. SUPPLEMENTARY NOTES		
19. KEY WORDS (Continue on reverse side if necessary and identify by block number)		
20. ABSTRACT (Continue on reverse side if necessary and identify by block number) Gas bubbles have been reported to routinely accumulate in cavities during anodic or cathodic polarization in several metals and alloys (Fe, Ni, Cu, Al, stainless steel). These in-place gas bubbles have been found to sharply increase the gradients of potential and ionic concentration within the cavities. A limiting electrode potential, E_{LM} , in the cavity has been observed, consistent with theoretical considerations which predict its existence. Mathematical modeling has been reasonably successful, especially in the case of cathodic polarization where the calculation shows that the potential and		

INSTRUCTIONS FOR PREPARATION OF REPORT DOCUMENTATION PAGE

RESPONSIBILITY. The controlling DoD office will be responsible for completion of the Report Documentation Page, DD Form 1473, in all technical reports prepared by or for DoD organizations.

CLASSIFICATION. Since this Report Documentation Page, DD Form 1473, is used in preparing announcements, bibliographies, and data banks, it should be unclassified if possible. If a classification is required, identify the classified items on the page by the appropriate symbol.

COMPLETION GUIDE

General. Make Blocks 1, 4, 5, 6, 7, 11, 13, 15, and 16 agree with the corresponding information on the report cover. Leave Blocks 2 and 3 blank.

Block 1. Report Number. Enter the unique alphanumeric report number shown on the cover.

Block 2. Government Accession No. Leave Blank. This space is for use by the Defense Documentation Center.

Block 3. Recipient's Catalog Number. Leave blank. This space is for the use of the report recipient to assist in future retrieval of the document.

Block 4. Title and Subtitle. Enter the title in all capital letters exactly as it appears on the publication. Titles should be unclassified whenever possible. Write out the English equivalent for Greek letters and mathematical symbols in the title (see "Abstracting Scientific and Technical Reports of Defense-sponsored RDT&E," AD-667 000). If the report has a subtitle, this subtitle should follow the main title, be separated by a comma or semicolon if appropriate, and be initially capitalized. If a publication has a title in a foreign language, translate the title into English and follow the English translation with the title in the original language. Make every effort to simplify the title before publication.

Block 5. Type of Report and Period Covered. Indicate here whether report is interim, final, etc., and, if applicable, inclusive dates of period covered, such as the life of a contract covered in a final contractor report.

Block 6. Performing Organization Report Number. Only numbers other than the official report number shown in Block 1, such as series numbers for in-house reports or a contractor grantees number assigned by him, will be placed in this space. If no such numbers are used, leave this space blank.

Block 7. Author(s). Include corresponding information from the report cover. Give the name(s) of the author(s) in conventional order (for example, John R. Doe or, if author prefers, J. Robert Doe). In addition, list the affiliation of an author if it differs from that of the performing organization.

Block 8. Contract or Grant Number(s). For a contractor or grantees report, enter the complete contract or grant number(s) under which the work reported was accomplished. Leave blank in in-house reports.

Block 9. Performing Organization Name and Address. For in-house reports enter the name and address, including office symbol, of the performing activity. For contractor or grantees reports enter the name and address of the contractor or grantees who prepared the report and identify the appropriate corporate division, school, laboratory, etc., of the author. List city, state, and ZIP Code.

Block 10. Program Element, Project, Task Area, and Work Unit Numbers. Enter here the number code from the applicable Department of Defense form, such as the DD Form 1498, "Research and Technology Work Unit Summary" or the DD Form 1634, "Research and Development Planning Summary," which identifies the program element, project, task area, and work unit or equivalent under which the work was authorized.

Block 11. Controlling Office Name and Address. Enter the full, official name and address, including office symbol, of the controlling office. (Equates to funding sponsoring agency. For definition see DoD Directive 5200.20, "Distribution Statements on Technical Documents.")

Block 12. Report Date. Enter here the day, month, and year or month and year as shown on the cover.

Block 13. Number of Pages. Enter the total number of pages.

Block 14. Monitoring Agency Name and Address (if different from Controlling Office). For use when the controlling or funding office does not directly administer a project, contract, or grant, but delegates the administrative responsibility to another organization.

Blocks 15 & 15a. Security Classification of the Report: Declassification/Downgrading Schedule of the Report. Enter in 15 the highest classification of the report. If appropriate, enter in 15a the declassification/downgrading schedule of the report, using the abbreviations for declassification/downgrading schedules listed in paragraph 4-207 of DoD 5200.1-R.

Block 16. Distribution Statement of the Report. Insert here the applicable distribution statement of the report from DoD Directive 5200.20, "Distribution Statements on Technical Documents."

Block 17. Distribution Statement of the abstract entered in Block 20, if different from the distribution statement of the report. Insert here the applicable distribution statement of the abstract from DoD Directive 5200.20, "Distribution Statements on Technical Documents."

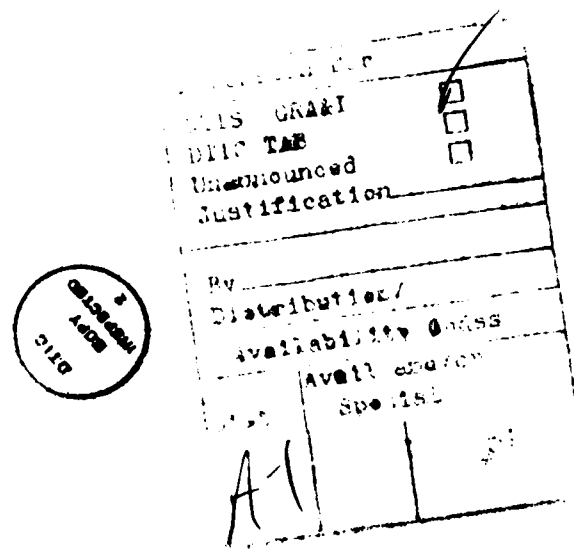
Block 18. Supplementary Notes. Enter information not included elsewhere but useful, such as: Prepared in cooperation with . . . Translation of (or by) . . . Presented at conference of . . . To be published in . . .

Block 19. Key Words. Select terms or short phrases that identify the principal subjects covered in the report, and are sufficiently specific and precise to be used as index entries for cataloging, conforming to standard terminology. The DoD "Thesaurus of Engineering and Scientific Terms" (TEST, AD-672 000, can be helpful).

Block 20. Abstract. The abstract should be a brief (not to exceed 200 words) factual summary of the most significant information contained in the report. If possible, the abstract of a classified report should be unclassified and the abstract to an unclassified report should consist of publicly-releasable information. If the report contains a significant bibliography or literature survey, mention it here. For information on preparing abstracts see "Abstracting Scientific and Technical Reports of Defense-Sponsored RDT&E," AD-667 000.

20. ABSTRACT continued

concentration gradients are strong functions of the "sharpness" of the crack, the ohmic voltage increasing as the crack opening decreases, in agreement with earlier calculations of current distribution in slots by Wagner. By analogy, a similar result is expected for anodic polarization. The shift of the potential with increasing distance into a cavity is always in the direction of a decrease in anodic or cathodic polarization, is typically very large approaching the E_{LIM} value of the system, is largely independent of the cathodic or anodic polarization, is typically very large approaching the E_{LIM} value of the system, is largely independent of the cathodic or anodic polarization applied to the external surface and often places that base of the cavity in a potential regime of other reactions, e.g., anodic metal dissolution at the crack tip while the sample's outer surface is under effective cathodic protection.



THE EFFECT OF GAS BUBBLES AND CAVITY DIMENSIONS ON THE LOCAL
ELECTRODE POTENTIAL WITHIN PITS, CREVICES AND CRACKS

BY

H. W. Pickering

Technical Report
to
Office of Naval Research
Contract NO. N000-14-81-K-0025

November 1983

Introduction

Some years ago Pickering and Frankenthal (1) found that gas accumulated inside growing pits while the sample was anodically polarized in the passive region. This observation was aided by (i) the use of a low power microscope, (ii) the fact that in the acidic electrolyte the formation of solid corrosion products was suppressed, (iii) the formation of "open", hemispherically-shaped pits, and (iv) the use of a glass fiber to probe inside the pit. This observation had to be important since at the very least the kinetics of pit growth, and possibly the mechanism, would be affected by the presence of a major obstruction within the pit. Its importance was all the more accentuated when the local electrode potential at the base of the pit was found by direct measurement to shift, typically hundreds of mV, in the less noble direction, often putting the base of the pit in the normal active region of the polarization curve for the bulk electrolyte. Few of the earlier theories of pit growth and crevice attack included large potential gradients within the growing pit or crevice. In contrast, our studies have been largely motivated by the possibility that the value of the local electrode potential may be an important factor in causing pit and crevice growth.

What is needed is a systematic study of the relationship between potential gradients and accumulating gas in the cavities, and of their importance in the pit and crevice growth processes. In addition, mathematical modeling of these anodic processes should include the occurrence of the reaction on the side walls. When this was done in the modeling of cathodic polarization in crevices (2), it introduced the spacing between the crack walls (crack "opening") as an important parameter, in agreement with earlier calculations by Wagner (3) which showed that narrowness of the electrolyte path affected the current distribution in slots. By analogy, the same result is expected during anodic polarization, i.e., the ohmic voltage increases in the crack (to a limiting* value) as the crack opening decreases. Thus, it seems likely in the case of sharp (closed) cracks, that during anodic polarization the local electrode potential at the crack tip will have a much less noble value and be in the active region while the sample's outer surface is in the passive region even without accumulation of gas in the crack.

It is the limited purpose of the present paper to focus on the effect of accumulating gas in the cavity and of the cavity dimensions on the value of the local electrode potential at the base of the cavity. Cathodic, rather than anodic polarization will be used for this part of the study since it provides a constant source of gas via the hydrogen evolution reaction (h.e.r.) and a control on the rate of gas accumulation in the cavity. In addition, mathematical modeling for cathodic polarization of creviced samples includes the occurrence of the h.e.r. on the crack walls (2). This feature in the model, in turn, leads to the above-mentioned important result that the potential gradient is a strong function of the crack opening. Another consequence of a cathodic polarization study is that the results will impact on the hydrogen cracking problem. Before proceeding

*The existence of a limiting potential, E_{LM} , has been proposed, and criteria which establish its value have been set forth (4). Some experimental evidence of its existence is also available in reference (2) and this paper.

to present a description of the conditions within cracks during cathodic polarization, the analogous situation of anodic polarization, will be reviewed in light of the early observation of in-place bubbles in pits and its significance for localized corrosion processes.

Anodic Polarization

In anodic-polarization measurements of the local electrode potential existing inside growing, gas-containing pits, the least noble, measured potential in the pit was typically at negative potentials in the active dissolution region (1). This was so even when the sample's outer surface was anodically polarized well into the passive region, e.g., > 1V (SHE). Hence, it was concluded that the simultaneously observed in-place gas bubbles which were identified as H₂ were the cause of these large (~10³ mV) changes in electrode potential within the iron cavity, and possibly also the cause of other earlier reported 10² to 10³ mV changes within pits in austenitic stainless steel (5) and carbon steel (6) which were largely inexplicable at the time. For these large IR drops the resistivity of the electrolyte was probably too low to account for this magnitude of ohmic voltage for the existing thickness of the electrolyte path and pitting current, without imposing factors which reduce the solution cross section available for carrying the current. On the other hand, for narrow crevices and large currents the cross section of the electrolyte path may be small enough to produce 10³ mV ohmic voltages within the crevice, as was suggested to explain other measured large ohmic voltages in titanium alloy (7) and stainless steel (8) although the calculations were not done.

Additional observations of accumulated gas within cavities also have been reported, including in the non ferrous alloys. In the case of Al, gas was observed to evolve from within the pits and found by analysis to be hydrogen (9). This observation of H₂ gas was not for the usual conditions of hydrogen evolution during pitting at open circuit, for which E_{CORR} < 0.0 V (SHE) and H₂ is evolved on the outer surface as the cathodic reaction (10,11). Rather, it was for anodic polarization to a potential (~2 V SHE) for which hydrogen evolution can not occur (at the outer surface), indicating that the local electrode potential in the pit was much less noble at a value below ~0.0 V (SHE).

The measured potential in the cavity will not usually be the least noble potential existing in the cavity. This value, which may approach E_{LIM}, is expected to be in the most confined regions, e.g., between the bubble and cavity wall and, therefore, not measurable without disturbing the bubble. The least noble measured local electrode potentials of -0.2 to 0.2 V (SHE) for Fe in different acidic solutions containing also Cl⁻ ion, which occur due to very effective constriction by in-place gas, are virtually independent of the extent of anodic polarization of the outer surface (1,4,12).

Measurement Technique

The potential measurement technique which utilizes a micro Luggin capillary probe has been found to be reliable and accurate to at least \pm 50 mV. This error limit was in part obtained from the following independent observations which confirm the reliability of the potential probe method.

(1) With the sample surface anodically polarized to potentials in the range 0.7 to 1.2 V (SHE), the gas forming within, and coming out of, growing pits in iron was analyzed as H₂. This places the local electrode potential in the pit at a value of <0.0 V, which is the most noble

equilibrium hydrogen potential possible at the base of the pits for any of the systems studied. The actual local electrode potential had to be more negative with its value dependent on the local h.e.r. current and pH. As mentioned above the most negative potentials within the pits would also be more negative than the measured values which were typically in the range, -0.2 to 0.2 V (1), in good agreement with the value of ~0.0 volts established by identification of the gas as hydrogen.

(2) In the same anodically polarized iron samples, ($E_{\text{surface}} = 0.7$ to 1.2 V) and also in anodically polarized stainless steel samples ($E_{\text{surface}} > 1.0$ V), the walls of the pits prior to salt film formation were observed to be crystallographically etched. Etched surfaces are typical of dissolution in the active region and, in particular, in the Tafel region. This would place the local electrode potential of the etched surface at less than approximately -0.2 V, which is also in good agreement with the measured values given above.

Mathematical Modeling

From a theoretical point of view, if the current path in the cavity is obstructed by the presence of gas bubbles, calculations of the IR voltage which are based on the geometrical cross section of the cavity will under-estimate the actual IR voltage. Many such calculations of the potential and concentration variations in pits and crevices available in the literature (1,12-16) all show that for an electrolyte which is a good conductor the ohmic voltage between the base and opening of a growing pit (or crack) is $\gtrsim 10^2$ mV. Even in the case of dilute (poorly conducting) electrolytes, the ohmic voltage in the cavity (in the absence of constrictions) may be quite small since the ionic concentration and, hence, the conductivity of the electrolyte within a growing pit or crevice, increases above that of the bulk solution (1). Measured values of the ohmic voltage in pits as reported above, are often an order of magnitude larger. Thus, a discrepancy exists between calculation and experiment. The cause of this discrepancy is the absence of a parameter in the model which takes into account a narrowing, e.g., due to accumulating gas, of the electrolyte path in the cavity.

On the other hand, if gas does not accumulate but narrowness is intrinsic in the form of localized corrosion, as in the case of a sharp crack, an appropriate model needs only to include this narrowness. By analogy with cathodic-polarization modeling (2), this would appear to mean inclusion of side wall dissolution in existing models. The anticipated results of such a model for anodic polarization may well show that potential changes for sharp cracks or narrow crevices, would be comparable to those produced in wide crevices or pits containing in-place gas bubbles.

Cathodic Polarization

Experimental

Following the above-mentioned anodic polarization behavior in cavities, large changes in electrode potential accompanied by accumulating gas were observed within crevice-like cavities during cathodic polarization (2,17). Figure 1 shows stable, in-place H₂ bubbles that typically form within crevices during the normal occurrence at a rate i of the h.e.r. on the sample surface. Simultaneously, as the in-place bubbles formed, the measured potential gradients within the crevices were found to markedly increase. The solution potential expressed in terms of $\phi_{x=0} = 0$, where $x=0$ is at the crevice mouth (Figure 6), is given in Figure 2 with and

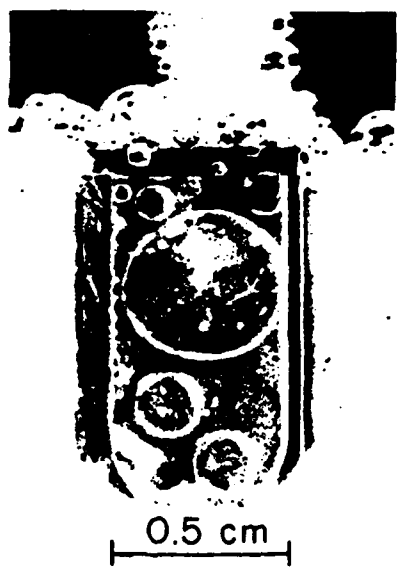


Figure 1. In-place hydrogen gas bubbles which formed during cathodic polarization at $i_s = 9 \text{ A m}^{-2}$, photographed through a transparent plastic which was used as one wall of the crevice. The other wall and outer surface were the iron sample. After Harris and Pickering (17).

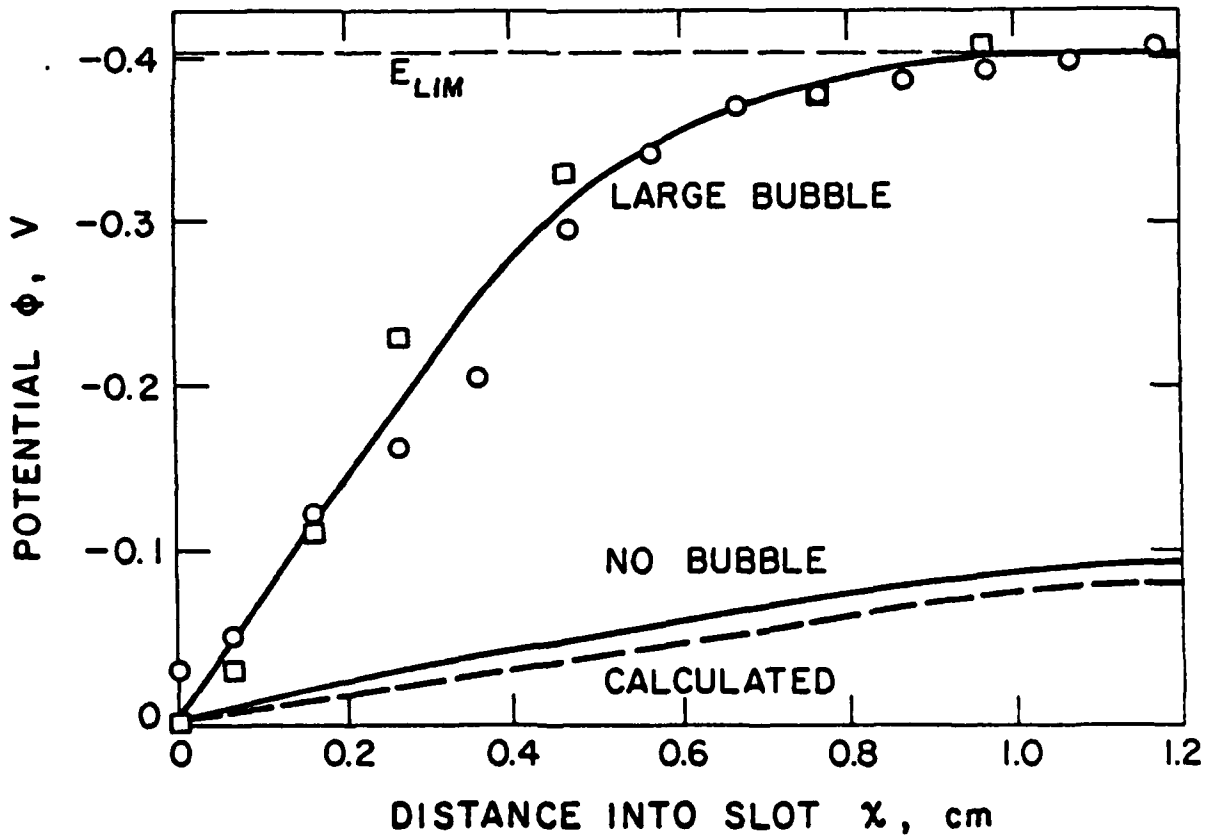


Figure 2. The measured potential profile as a function of distance x for crevices with and without bubbles during cathodic polarization at $i_s = 52 \text{ A m}^{-2}$. After Ateya and Pickering (2).

without in-place bubble formation. The upper curve corresponds to in-place bubbles of size comparable to the crevice cross section, as shown in Figure 1. For this situation the limiting potential, E_{LIM} , is reached near the bottom of the crevice ($x > 0.9$ cm).

The slot in Figure 1 was relatively large in terms of real crevices and very large in terms of most cracks. However, in spite of the openness of the slot, the bubbles readily formed and filled the cross section. Similarly, bubble formation has been routinely observed within crevice-like slots in Cu, Ni and Fe samples (2). In the latter observations, made from the crevice opening, a transparent plastic was not used so that it was clear that the formation and stability of the in-place bubbles within the crevices were characteristic of metal crevices and not of the plastic surface used for visual observation (Figure 1). Large potential gradients were measured in all of these samples when the crevices contained in-place gas bubbles, as shown in Table I.

Table I. The measured solution potential, $\phi_{x=L}$ and electrode potentials $E_{x=0}$ and $E_{x=L}$ where $x = 0$ at the crevice opening and $x=L$ at its bottom (2).

Metal	Solution	$i_s, A m^{-2}$	$E_{x=0} \text{ SHE, V}$	$\phi_{x=L} \text{ V}$	$E_{x=L} \text{ SHE, V}$	Estimated $E_{LIM} \text{ SHE, V}$
Fe	0.5M Acetate, 0.5M Acetic Acid, (pH=5)	50	-0.9	-0.4	-0.5	$E_{mixed} \approx -0.4$
Ni	1M HClO_4	100	-0.7	-0.5	-0.2	$E_{mixed} \approx -0.1$
Cu	1M HClO_4	100	-0.7	-0.5	-0.2	$E_{equil} \approx 0.0$

Below, and in the region of contact of the bubbles with the iron (Figure 1), the iron underwent anodic dissolution during effective cathodic protection of the sample's outer surface, as revealed by the etched condition of the crevice wall (originally polished) in Figure 3. Other

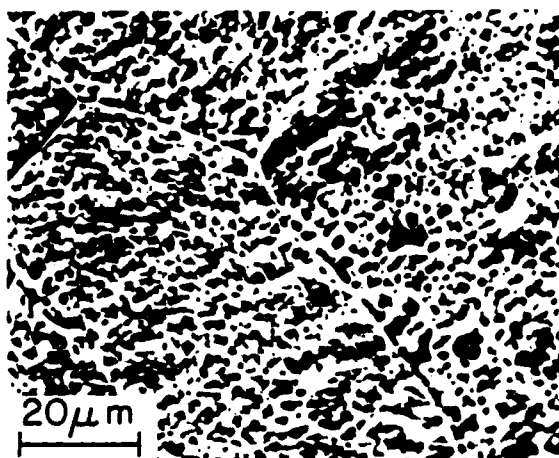


Figure 3. SEM micrograph illustrates etching of the crevice wall at the point of contact of the largest in-place bubble in Figure 1. After Harris and Pickering (17).

experiments were performed on the Fe, Ni and Cu samples to test for anodic dissolution within the crevices. In these experiments it was not possible to check for etching since the wall surfaces could not be polished prior to the experiment. Instead, solution was extracted from the crevice during the cathodic hydrogen evolution experiments, and analyzed for metal ions. The results of these analyses are shown in Table II. Estimated concentrations at the base of the crevices are also listed, and are much larger than the measured ("crevice") values in order to account for dilution of the crevice solution during extraction. In contrast to the dissolution of Fe and Ni in their crevices, the solution in the Cu crevice contained no copper ions within the accuracy of the measurement, in accord with the E_{LIM} condition as explained below.

Table II. The measured concentrations of Fe^{2+} , Ni^{2+} and Cu^{2+} ions in samples of electrolyte extracted from within crevices and from bulk solution for the h.e.r. currents and solution compositions shown in Table I. (2).

Metal	Bulk $[M^{2+}]$ (ppm)	"Crevice" $[M^{2+}]$ (ppm)	Estimated $[M^{2+}]$ @ $x=L$ (ppm)
Fe	2	50	≈ 5000
Ni	0.2	15	≈ 1000
Cu	---	1	---

The change in solution potential, ψ , given in Figure 2, is related to the local electrode potential, E_x , in the cavity by (3)

$$E_x = E_{x=0} - \psi_x \quad (1)$$

Inserting the largest (measured) value of solution potential ($\psi_{x=L} = -0.4V$) from Figure 2 and Table I, and the measured electrode potential at the outer surface ($E_{x=0} = -0.9V$), Eq. 1 yields $E_{x=L} = -0.5 V$ (SHE). This is the most noble measured electrode potential in the crevice and is located below the large bubble in Figure 1. Since it is in the vicinity of the standard potential of Fe, anodic dissolution of iron is expected in the crevice and was observed (Table II). Hence, the situation in the crevices of iron containing in-place gas bubbles is as shown in Figure 4 where the ψ potential is sufficiently large to shift the local electrode potential (beneath and in the vicinity of the bubble) into the potential region of iron dissolution. A mirror-symmetry of Figure 4 is shown in Figure 5 for anodic polarization. Because current flows out of the cavity for anodic polarization, the electrode potential in the cavity is less, rather than more, noble than the value at the outer surface. The idea of an active pit base with an electrode potential which is 10^2 to 10^3 mV less noble than that at the outer passive surface goes back to the early discussions of Uhlig (4) and subsequently others (1,12,18,19).

The limiting potential, E_{LIM} , is the potential in the slot for which the iron dissolution and hydrogen evolution currents are equal (E_{mixed} in Table I). At the corresponding depth and below (for $E_x = E_{LIM}$), current from the external polarization is essentially zero. However, it is finite to this depth so that, in principle, E_{LIM} can be reached for cathodic reactions, in contrast to those situations for anodic polarization where cavity growth, e.g., pit or crack, occurs by anodic metal dissolution at the pit base or crack tip. If E_{LIM} were to be reached for

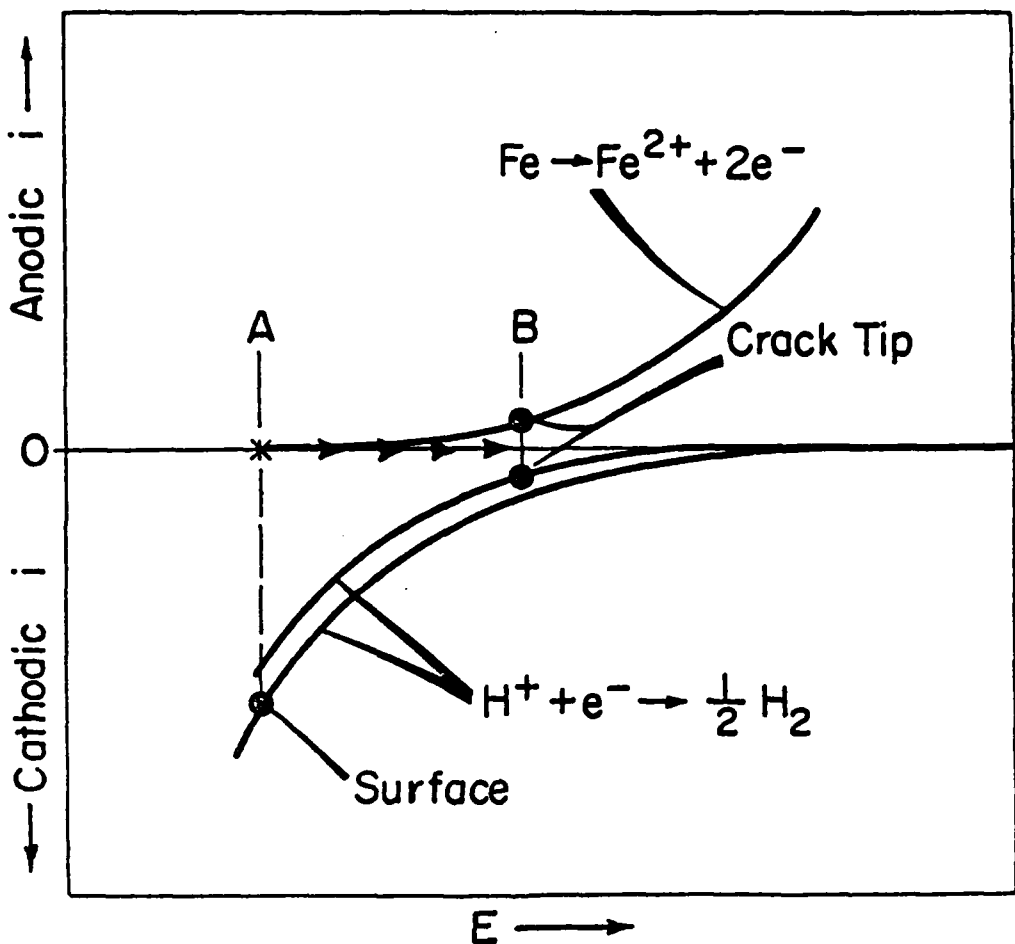


Figure 4. Schematic showing $E_{x=L}$ (at the bottom of the crack) approaching E_B in the potential region of iron dissolution for cathodic polarization of the outer surface at E_A (2,4,12). $E_{LIM} = E_B$.

the latter (E_B in Figure 5), there would be zero net current flowing out of the cavity in which case the ohmic voltage would be zero and a potential less noble than E_A could not be supported in the cavity (4). On the other hand if E_{LIM} were to be reached during cathodic polarization, a finite current could still flow into the cavity by virtue of the distribution of the h.e.r. on the side walls, and thereby maintain an ohmic voltage between the cavity opening and a depth into the cavity over which the h.e.r. occurs. Near, or at E_{LIM} the situation is probably closest to what early workers referred to as the "occluded cell" in describing pitting although most emphasized ionic concentration gradients and did not include ohmic voltages as significant since measurement of their magnitude were largely unavailable.

The situation for Ni is qualitatively the same as shown in Figure 4 for iron. The situation for Cu is different in that the copper anodic dissolution curve does not overlap the h.e.r. cathodic polarization curve. It follows that E_{LIM} for the crevice in Cu is the equilibrium potential for the h.e.r., E_{equil} (Table I), for the ionic concentrations existing in the crevice (4).

Mathematical Modeling

Mathematical modeling of the h.e.r. in crevices has been successful in the case of crevices free of gas (dashed curve in Figure 2). An important

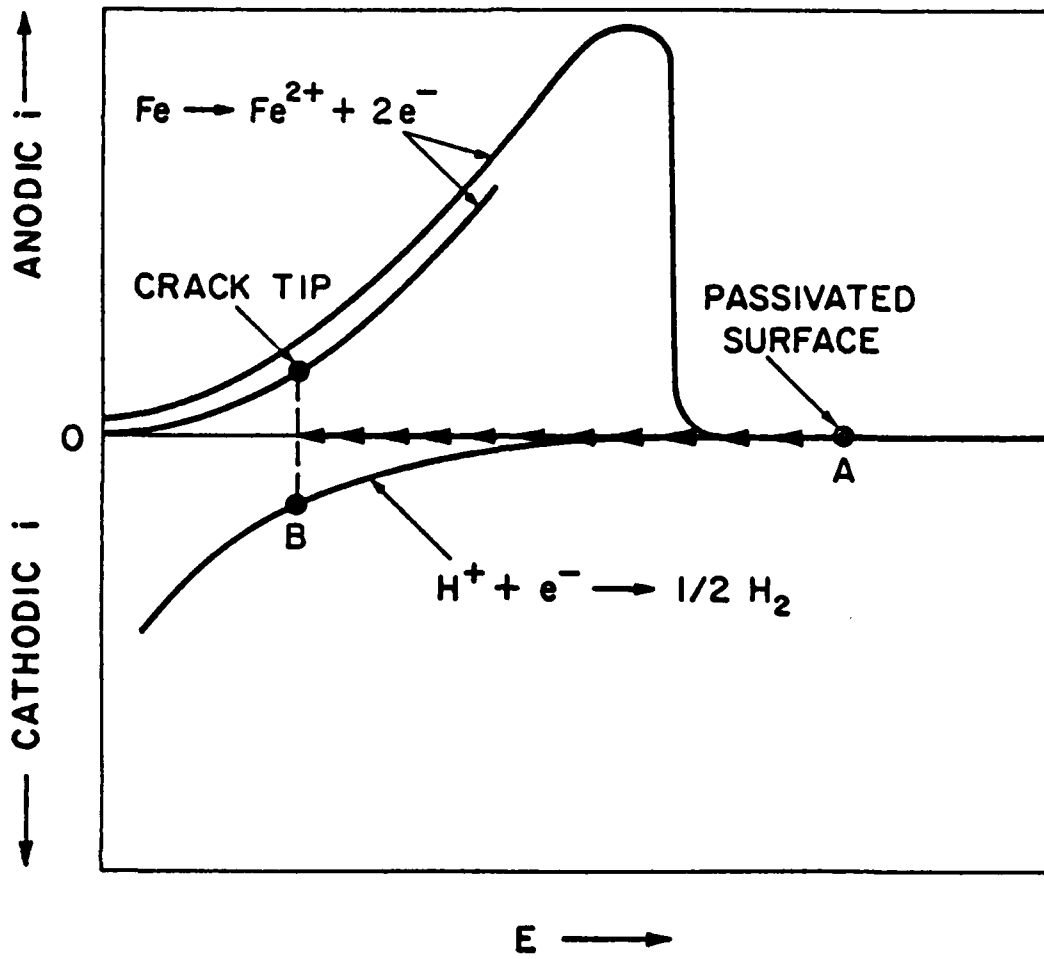


Figure 5. As in Figure 4 but for anodic polarization (1,3,5.12).
 $E_{x=L}$ approaches E_B for $E_{x=0} = E_A$ (4). $E_{\text{LIM}} = E_B$.

feature of these models is that they include the h.e.r. on the crevice walls and treat it as an unknown in the calculation (2). Let us consider the h.e.r. in a simple strong acid HY of monovalent ions and a crevice geometry shown in Figure 6. The cross section of the crevice is a rectangle of thickness α and width b , and its depth is L such that $\alpha \ll L$ and $\alpha \ll b$, in which case the h.e.r. can be considered to occur only on the outer surface and on the crevice (or crack) walls. A more precise condition for validity of the equations is $X \gg \alpha$ where X is a characteristic distance defined below.

The fluxes, j , of the H^+ and Y^- ions in the x direction within the crevice/crack are

$$j_{H^+} = -D_{H^+} \left(\frac{dc_{H^+}}{dx} + c_{H^+} \frac{F}{RT} \frac{d\phi}{dx} \right) = \frac{i}{F} \quad (2)$$

$$j_{Y^-} = -D_{Y^-} \left(\frac{dc_{Y^-}}{dx} - c_{Y^-} \frac{F}{RT} \frac{d\phi}{dx} \right) = 0 \quad (3)$$

where D and c are the diffusivity and concentration of the indicated species, respectively, ϕ is the solution potential with respect to $\phi = 0$ at $x = 0$, and i is the (unknown) current density distribution on the crack walls for the impressed h.e.r. current on the sample surface, i_s . The

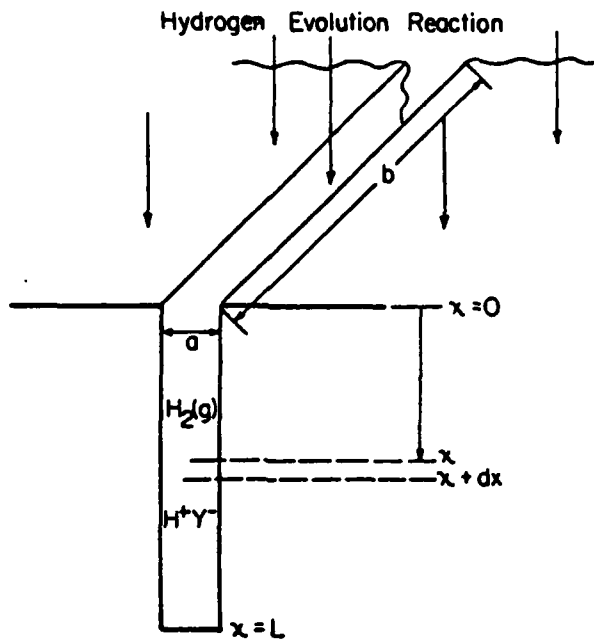


Figure 6. Model of crack.

electroneutrality equation is

$$c_{H^+} = c_{Y^-} = c \quad (4)$$

The boundary condition at $x=0$ for a bulk acid concentration of c_0 is

$$c_{H^+} = c_{Y^-} = c_0 \text{ and } \psi \equiv 0 \text{ at } x=0 \quad (5)$$

A boundary condition at $x = L$ evolves from the calculation which can be found elsewhere (2). Equations (2) to (5) are then used to obtain ψ , c_{H^+} , c_{Y^-} and i as functions of x , c_0 , a and i_s .

The characteristic length X is obtained as (2)

$$X = (D_{H^+} c_0 F a / i_s)^{1/2} \quad (6)$$

and the solutions for the unknowns are

$$\psi = \frac{RT}{F} \ln \frac{\cosh [(L-x)/X]}{\cosh [L/X]} \quad (7)$$

$$c_{H^+} = c_{Y^-} = c_0 \frac{\cosh [(L-x)/X]}{\cosh [L/X]} \quad (8)$$

$$i = i_s \frac{\cosh [(L-x)/X]}{\cosh [L/X]} \quad (9)$$

Equations (7) and (1) may be used to estimate the depth at which the electrode potential assumes a sufficiently noble value for anodic dissolution of the metal, within the constrain of E_{LM} . Equations (8) and (9) may be used to estimate the depth at which depletion of H^+ and decrease in the hydrogen evolution rate became significant, e.g., the depth corresponding to the equilibrium pH of the hydrolysis reaction. Equation (7) is the dashed curve in Figure 2 and compares well with the measured curve (lower solid curve) for experimental conditions which, although not exactly matching the model conditions, are for a bubble-free crevice.

One of the most important features of Equation (7) using also Equation (6) is that it includes the slot "openness", α , in its solution. Thus, evaluation of Equation (7) shows that ϕ becomes more negative as the crack dimension α decreases, and from Equation (1) E_x becomes more noble. This strong effect of the crack openness on the local solution potential in Equation (7) is plotted in Figure 7. It shows that in the case of "sharp" cracks ($\alpha \approx 50 \mu\text{m}$) very large (negative) ϕ values are to be expected. This is quite a different situation than for most other models of mass transport for cathodic or anodic polarization, which do not show a strong relation between the ohmic voltage and the openness of the crack or crevice. Thus, the salient point is that this model successfully predicts large (10^2 to 10^3 mV) ohmic voltages without incorporating constrictions such as gas bubbles in the cavity, but only for sharp, closed cracks, e.g., $\alpha \approx 50 \mu\text{m}$ for $i_s = 100 \text{ A m}^{-2}$. For more open cracks or crevices, the 10^2 to 10^3 mV measured ohmic voltages can only be accounted for by the presence of constrictions in the cavity. Similarly, Equations 8 and 9 show that the concentration and current-density gradients also become steeper as α decreases, as shown in Figures 8 and 9, respectively.

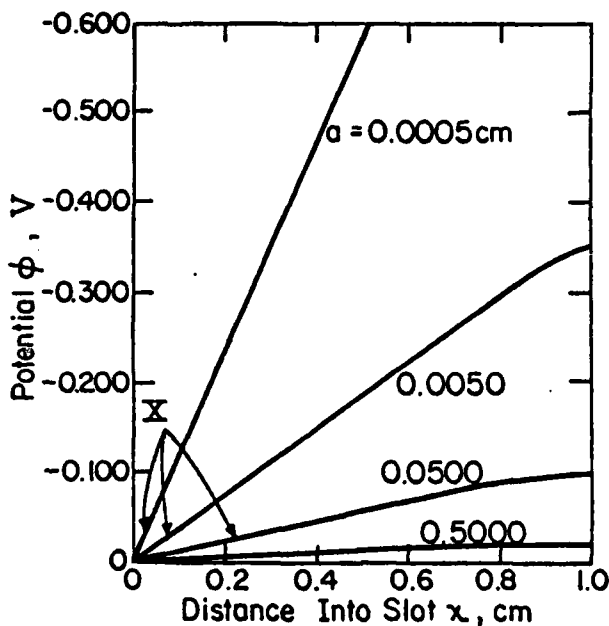


Figure 7. Effect of crack "openness", α , on the solution-potential profile inside a crack of depth $L = 1 \text{ cm}$ for $i_s = 100 \text{ A m}^{-2}$ (2).

Conclusions

This paper reviews and elaborates on the relation between the local electrode potential in cavities and two parameters; accumulated gas in the cavity and the narrowness of the electrolyte path, e.g., the sharpness of a crack. It does this by considering experimental and theoretical results for both anodic and cathodic polarization. The discussion includes and elaborates on the limiting electrode potential within cavities.

The following observations are made:

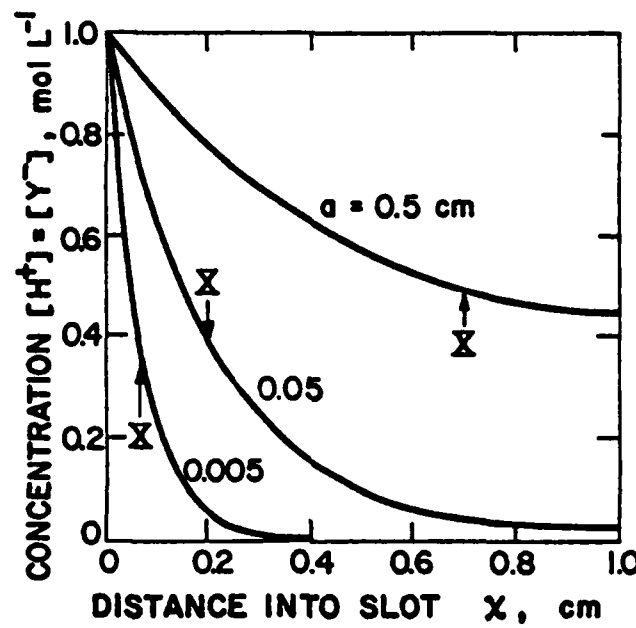


Figure 8. As in Figure 7 but illustrating the effect of α on the concentration gradients of H^+ and Y^- ions within the slot (2).

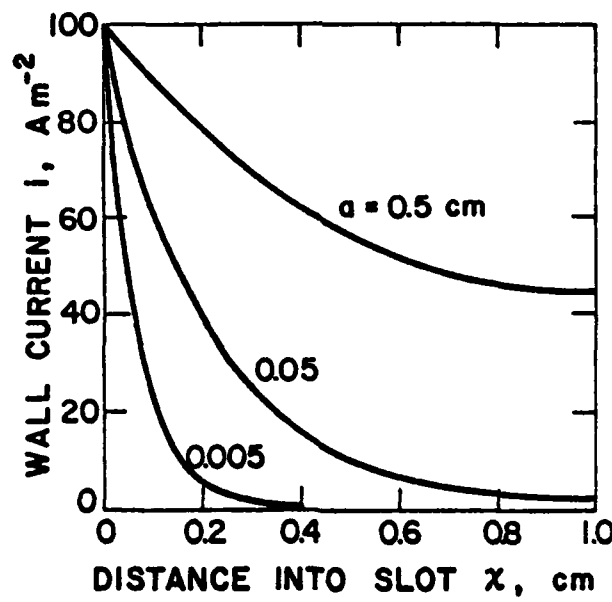


Figure 9. As in Figure 7 but illustrating the effect of α on the current distribution of the h.e.r. on the slot walls (2).

- (1) Ohmic voltages of several hundred mV which have been measured in growing pits, wide crevices or open cracks can not be explained by simply considering the resistivity of the solution as was suggested in much of the early literature.
- (2) Two explanations of these large ohmic voltages exist. Both rely on making the cavity very narrow. In the case of "open" cavities (pits, crevices or cracks), gas or possibly solid corrosion product accumulation in the cavity is important. In the case of sharp cracks or crevices, narrowness is intrinsic in the form of corrosion (small a in Figure 6) and can be adequate, by itself, i.e., without involving constrictions, to produce large (10^2 to 10^3 mV) ohmic voltages.
- (3) For sharp cracks or gas-filled pits or crevices the local electrode potential may approach or equal the limiting potential, E_{LM} , and be largely independent of the applied (anodic or cathodic) polarization at the external surface of the sample.
- (4) Reactions in cavities are a function of the local electrode potential and solution composition and may be different than those at the external surface e.g., metal dissolution may occur at a crack tip during effective cathodic protection of its outer surface.

Acknowledgement

Financial support by the Office of Naval Research under Contract No. N00014-81-K-0025 and by CONICIT, Venezuela, (A.V.) is gratefully acknowledged.

References

1. H. W. Pickering and R. P. Frankenthal, J. Electrochem. Soc., 119, (1972) pp. 1297-1310.
2. B. G. Ateya and H. W. Pickering, J. Electrochem. Soc., 122, (1975) pp. 1018-1026.
3. C. Wagner, Plating, 48 (1961) pp. 997-1002.
4. H. W. Pickering, "The Limiting IR Voltage Within Electrolyte in Cavities during Localized Corrosion and Hydrogen Charging of Metals", pp. 85-91 in H. H. Uhlig Symposium, Corrosion and Corrosion Protection, R. P. Frankenthal and F. Mansfeld, eds., The Electrochem. Soc., Inc., Pennington, N.J., 1981.
5. H. H. Uhlig, The Corrosion Handbook, p. 165, Wiley and Sons, Inc., New York, N.Y., 1948.
6. G. Herbsleb and H. J. Engell, Z. Elektrochem., 65, (1961) pp. 881-887; Werkstoffe und Korrosion, 17, (1966) pp. 365-376.
7. C. M. Chen, F. H. Beck and M. G. Fontana, Corrosion, 27, (1971) pp. 234-238.
8. N. D. Greene, W. D. France, Jr., and B. E. Wilde, Corrosion, 21, (1965) pp. 275-276.
9. C. B. Bargeron and R. C. Benson, J. Electrochem. Soc., 172, (1980) pp. 2528-2530.
10. H. Kaesche, Korrosion, 16, (1963) p. 17; Z. Phys. Chem. N.F., 34, (1962) p. 114.
11. W. R. Fisher, Tech. Mitt. Krupp, 22, (1964) p. 125.

12. B. G. Ateya and H. W. Pickering, "Electrochemical Processes Within Cavities and Their Relation to Pitting and Cracking", pp. 206-222 in Hydrogen in Metals, I. M. Bernstein and A. W. Thompson, ed; ASM, Metals Park, OH, 1974.
13. T. R. Beck and E. A. Grens II, J. Electrochem. Soc., 116 (1969) pp. 177-184.
14. B. G. Ateya and H. W. Pickering, "Effect of Mass Transfer in the Aqueous Phase on Repassivation of Activated Surfaces and the Stability of Protective Films", pp. 350-367 in Passivity of Metals, R. P. Frankenthal and Jerome Kruger, eds., The Electrochem. Soc., Inc., Pennington, N. J., 1978.
15. R. Alkire, D. Ernsberger and D. Damon, J. Electrochem. Soc., 123 (1976). pp. 458-464.
16. J. R. Galvele, J. Electrochem. Soc., 123, (1976) pp. 464-474.
17. D. Harris and H. W. Pickering, "On Anodic Cracking During Cathodic Hydrogen Charging," pp. 229-231 in Effect of Hydrogen on the Behavior of Materials, A. W. Thompson, I. M. Bernstein, and A. J. West, ed; AIME, Warrendale, Pa., 1976.
18. W. Schwenk, Corrosion, 20 (1964) pp. 129t-137t.
19. U. R. Evans, The Corrosion and Oxidation of Metals, Supplement 2, p. 126, Edward Arnold Ltd., London, 1976.

BASIC DISTRIBUTION LIST

Technical and Summary Reports November 1979

<u>Organization</u>	<u>Copies</u>	<u>Organization</u>	<u>Copies</u>
Defense Documentation Center Cameron Station Alexandria, VA 22314	12	Naval Air Propulsion Test Center Trenton, NJ 08628 ATTN: Library	1
Office of Naval Research Department of the Navy 800 N. Quincy Street Arlington, VA 22217 ATTN: Code 471 Code 470	1	Naval Construction Battalion Civil Engineering Laboratory Port Hueneme, CA 93043 ATTN: Materials Division	1
Commanding Officer Office of Naval Research Branch Office Building 114, Section D 666 Summer Street Boston, MA 02210	1	Naval Electronics Laboratory San Diego, CA 92152 ATTN: Electron Materials Sciences Division	1
Commanding Officer Office of Naval Research Branch Office 536 South Clark Street Chicago, IL 60605	1	Naval Missile Center Materials Consultant Code 3312-1 Point Mugu, CA 92041	1
Naval Research Laboratory Washington, DC 20375 ATTN: Codes 6000 6100 6300 2627	1 1 1 1	Commanding Officer Naval Surface Weapons Center White Oak Laboratory Silver Spring, MD 20910 ATTN: Library	1
Naval Air Development Center Code 606 Warminster, PA 18974 ATTN: Dr. J. Deluccia	1	Commander David W. Taylor Naval Ship Research and Development Center Bethesda, MD 20084	1
		Naval Oceans Systems Center San Diego, CA 92132 ATTN: Library	1
		Naval Underwater System Center Newport, RI 02840 ATTN: Library	1
		Naval Postgraduate School Monterey, CA 93940 ATTN: Mechanical Engineering Department	1
		Naval Weapons Center China Lake, CA 93555 ATTN: Library	1

BASIC DISTRIBUTION LIST (cont'd)

<u>Organization</u>	<u>Copies</u>	<u>Organization</u>	<u>Copies</u>
Naval Air Systems Command Washington, DC 20360 ATTN: Codes 52031 52032	1	NASA Lewis Research Center Lewis Research Center 21000 Brookpark Road Cleveland, OH 44135 ATTN: Library	1
Naval Sea System Command Washington, DC 20362 ATTN: Code OSR	1	National Bureau of Standards Washington, DC 20234 ATTN: Metals Sience and Standards Division Ceramics Glass and Solid State Science Division Fracture and Deformation Division	1
Naval Facilities Engineering Command Alexandria, VA 22331 ATTN: Code 03	1	Director Applied Physics Laboratory University of Washington 1013 Northeast Forthieth Street Seattle, WA 98105	1
Scientific Advisor Commandant of the Marine Corps Washington, DC 20380 ATTN: Code AX	1	Defense Metals and Ceramics Information Center Battelle Memorial Institute 505 King Avenue Columbus, OH 43201	1
Army Research Office P.O. Box 12211 Triangle Park, NC 27709 ATTN: Metallurgy & Ceramics Program	1	Metals and Ceramics Divison Oak Ridge National Laboratory P.O. Box X Oak Ridge, TN 37380	1
Army Materials and Mechanics Research Center Watertown, MA 02172 ATTN: Research Programs Office	1	Los Alamos Scientific Laboratory P.O. Box 1663 Los Alamos, NM 87544 ATTN: Report Librarian	1
Air Force Office of Scientific Research/NE Building 410 Bolling Air Force Base Washington, DC 20332 ATTN: Chemical Science Directorate Electronics & Materials Sciences Directorate	1	Argonne National Laboratory Metallurgy Division P.O. Box 229 Lemont, IL 60439	1
AFWAL/MLL Wright-Patterson AFB Dayton, OH 45433	1	Brookhaven National Laboratory Technical Information Division Upton, Long Island New York 11973 ATTTN: Research Library	1
Library Building 50, Room 134 Lawrence Radiation Laboratory Berkeley, CA 94700	1	Office of Naval Research Branch Office 1030 East Green Street Pasadena, CA 91106	1
NASA Headquarters Washington, DC 20546 ATTN: Code RRM	1		

SUPPLEMENTARY DISTRIBUTION LIST

Technical and Summary Reports

Dr. T. R. Beck
Electrochemical Technology Corporation
31st Avenue, NE
Seattle, Washington 98125

Professor I. M. Bernstein
Carnegie-Mellon University
Schenley Park
Pittsburgh, Pennsylvania 15213

Professor H. K. Birnbaum
University of Illinois
Department of Metallurgy
Urbana, Illinois 61801

Dr. Otto Buck
Rockwell International
1049 Camino Dos Rios
P.O. Box 1085
Thousand Oaks, California 91360

Dr. W. Morris
Rockwell International
1049 Camino Dos Rios
P.O. Box 1085
Thousand Oaks, California 91360

Dr. David L. Davidson
Southwest Research Institute
8500 Culebra Road
P.O. Drawer 28510
San Antonio, Texas 78284

Dr. D. J. Duquette
Department of Metallurgical Engineering
Rensselaer Polytechnic Institute
Troy, New York 12181

Professor R. T. Foley
The American University
Department of Chemistry
Washington, D. C. 20016

Dr. J. A. S. Green
Martin Marietta Corporation
1450 South Rolling Road
Baltimore, Maryland 21227

Professor R. H. Heidersbach
University of Rhode Island
Department of Ocean Engineering
Kingston, Rhode Island 02881

Professor H. Herman
State University of New York
Material Sciences Division
Stony Brook, New York 11790

Professor J. P. Hirth
Ohio State University
Metallurgical Engineering
1314 Kinnear Road
Columbus, Ohio 43212

Professor R. M. Latanision
Massachusetts Institute of Technology
77 Massachusetts Avenue
Room E19-702
Cambridge, Massachusetts 02139

Dr. F. Mansfield
Rockwell International Science Center
1049 Camino Dos Rios
P.O. Box 1085
Thousand Oaks, California 91360

Dr. Jeff Perkins
Naval Postgraduate School
Monterey, California 93940

Dr. E. A. Starke, Jr.
Georgia Institute of Technology
School of Chemical Engineering
Atlanta, Georgia 30332

Dr. R. P. Wei
Lehigh University
Institute for Fracture and
Solid Mechanics
Bethlehem, PA 18015

SUPPLEMENTARY DISTRIBUTION LIST (continued)

Professor H. G. F. Wilsdorf
University of Virginia
Department of Materials Science
Charlottesville, Virginia 22903

Dr. Clive Clayton
State University of New York
Material Sciences Division
Stony Brook, New York 11970

Dr. Henry Leidheiser
Center for Surface and Coatings Research
Sinclair Memorial Laboratory 7
Lehigh University
Bethlehem, PA 18015

Prof. Morris E. Fine
Northwestern University
The Technological Institute
Evanston, IL 60201

Dr. C. S. Kortovich
TRW, Inc.
2355 Euclid Avenue
Cleveland, OH 44117

Dr. J. Kruger
National Bureau of Standards
Washington, DC 20234

Dr. Barry C. Syrett
Stanford Research Institute
333 Ravenswood Avenue
Menlo Park, CA 94025

Prof. S. Weissmann
Rutgers, The State University
of New Jersey
College of Engineering
New Brunswick, NJ 08903

Dr. R. J. Arsenault
University of Maryland
College Park, MD 20742

Prof. A. J. Ardell
University of California
School of Engineering & Applied Science
405 Hilgard Ave.
Los Angeles, CA 90024

Prof. J. G. Byrne
The University of Utah
Dept. of Materials Science & Engineering
Salt Lake City, Utah 84112

Prof. Alexander M. Cruickshank
Gordon Research Conference
Pastore Chemical Laboratory
University of Rhode Island
Kingston, RI 02881

Dr. Paul Gordon
Illinois Institute of Technology
Department of Metallurgical and Materials
Engineering
Chicago, IL 60616

Dr. J. V. McArdell
University of Maryland
College Park, MD 20742

Dr. E. McCafferty
Naval Research Laboratory
Washington, DC 20375

Prof. G. H. Meier & F. S. Pettit
University of Pittsburgh
Dept. of Metallurgical and Materials
Engineering
Pittsburgh, PA 15261

END

FILMED

12-83

DWIC